Visualization of human cognitive processing by MEG

Sunao Iwaki[1], Giorgio Bonmassar[2], John W Belliveau[2]*

[1]Human Technology Research Institute, National Institute of Advanced Industrial Science and Technology (AIST), AIST Tsukuba Central 6, 1-1-1 Higashi, Tsukuba 305-8566, Japan.
s.iwaki@aist.go.jp

[2]Athinoula Martinos Center for Biomedical Imaging, Massachusetts General Hospital (MGH), Bldg. 149, 13th St. Charlestown, MA 02129, USA.

Abstract

Each non-invasive neuroimaging technique has its own inherent limitations resulting from temporal and special inaccuracies due to the nature of information that can be measured. While functional magnetic resonance imaging (fMRI) provides excellent spatial localization of the brain activity up to sub-millimeter resolution, its temporal resolution is limited by the hemodynamic time constant. Conversely, magnetoencephalography (MEG), which measure temporal changes in neural current directly, has temporal resolution of a few milliseconds; however, its spatial accuracy is limited by the non-uniqueness of the biomagnetic inverse problem in which the spatial distribution of neural currents is estimated from the MEG field distributions outside of the head. In this paper, recent developments in multimodal neuroimaging are introduced to allow for the reconstruction of human brain dynamics with high spatial accuracy without compromising temporal resolution. Specifically, we describe a technique to combine data from MEG, MRI and fMRI to visualize human higher order visual processing while perceiving a three-dimensional (3-D) shape from two-dimensional (2-D) motion.

1. Introduction

Information processing, which takes place in neural networks in human cerebral cortical areas, plays a key role in perception, cognition, attention, memory and language. To investigate these crucial functions in the human brain, several noninvasive techniques were recently developed. However, none of these noninvasive techniques is capable of achieving sufficient temporal and spatial resolution at the same time to illustrate precise neural dynamics taking place in the living human brain.

Functional magnetic resonance imaging (fMRI) makes it possible to precisely visualize the spatial distribution of human brain activity with a resolution that is typically approximately a few millimeters. However, fMRI measures hemodynamic changes (blood oxygenation level dependent (BOLD) signals) [1, 2], which are an indirect measure of neural activity. These changes peak a few seconds after the onset of neural firing in an area, and therefore, this technique has limited temporal resolution.

Although magnetoencephalography (MEG) can record temporal changes of post-synaptic neural activity with good temporal resolution (on the order of milliseconds) [3], the principal difficulty in interpreting MEG data is in reconstructing the spatial distribution of the neural activity in the brain from MEG field distributions measured at sensors located at a distance from the brain area from which activity is being assessed. Because of the difficulty of solving this problem, we have to introduce prior knowledge of brain activity to obtain a unique solution [3]. This paper describes a technique to utilize three-dimensional structural models of the human brain derived from structural MRI scans [4] and spatial distributions of brain activity from functional MRI scans [5] to impose neurophysiologically plausible constraints on the MEG inverse problem.

2. fMRI Incorporated MEG Inverse Procedure

Introducing prior spatial imaging information into the MEG inverse problem, based on neuroimaging modalities such as fMRI, could significantly improve the spatial accuracy of the inverse problem, assuming that the local BOLD response measured by fMRI is highly correlated in the adjacent region with post-synaptic neuronal activity, which is the major source of MEG signals. In fact, previous studies that simultaneously used intracortical neuroelectric recordings (local field potential: LFP) and BOLD signals on primates revealed a tight coupling between local neural activity and BOLD responses [6]. These results suggest that maps of brain activity obtained by fMRI experiments, in which a set of

978-1-4673-5225-3/14/$31.00 ©2014 IEEE

tasks for MEG experiments are first imaged using fMRI, can be used as a reference template spatial map prior to solving the MEG inverse problem.

Here, we define the primary current distribution, which is a major generator of MEG signals, as $\mathbf{p} = [p_1, p_2, \ldots, p_N]$, and the measured distribution of MEG as $\mathbf{b} = [b_1, b_2, \ldots, b_M]$ where M is the total number of possible neural current sources in the brain and N is the number of sensors. According to the Maxwell equation for quasi-static electromagnetic fields and the Biot-Savart law [3], **b** is related to **p** as shown in equation (1). By introducing an M-by-N gain matrix **L**, which is called the lead field matrix, describing a geometric relationship between the possible source locations and the sensor locations or a sensitivity distribution of each sensor.

$$\mathbf{b} = \mathbf{L}\,\mathbf{p} + \mathbf{n} \tag{1}$$

where **n** is the noise obtained when acquiring data.

In equation (1), the number of possible neural current sources (N) is typically on the order of thousands, whereas the typical number of MEG sensors (M) is at most on the order of hundreds. Hence, we have to estimate thousands of parameters using only hundreds of linear equations. In the traditional inverse formulation, a "minimum-norm constraint" is commonly employed where the least norm solution is selected from among the possible set of solutions (minimum-norm estimates: MNE) [7]. The MNE of the neural current distribution ($\hat{\mathbf{p}}$) is given by

$$\hat{\mathbf{p}} = \boldsymbol{L}^{-}\,\mathbf{b} \tag{2}$$

where the generalized inverse of the lead field matrix ($\boldsymbol{L}^{-}$) is written as [8]

$$\mathrm{L}^{-} = (\mathrm{W}\,\mathrm{W}^{\mathrm{T}})^{-1}\mathrm{L}^{\mathrm{T}}(\,\mathrm{L}\,(\mathrm{W}\,\mathrm{W}^{\mathrm{T}})^{-1}\mathrm{L}^{\mathrm{T}} + \gamma^2\mathrm{I})^{-1} \tag{3}$$

The diagonal matrix **W** contains the weighting factors in the solution space, and γ is a regularization parameter, which controls the degree of regularization, determined in accordance with the signal-to-noise ratio of measurements. By employing the generalize inverse operator in eq (3), the solution $\hat{\mathbf{p}}$ that minimizes the objective function,

$$E = \left\|\mathbf{b} - \hat{\mathbf{b}}\right\|^2 + \gamma^2\|\mathbf{W}\ \hat{\mathbf{p}}\|^2 \tag{4}$$

is selected for the reconstructed current distribution. The prior spatial information on the neural activity distribution could be introduced by modifying the weighting factor **W** so that the weights "guide" the solution toward the areas of significant fMRI activation ([9] for detailed formulation).

3. Application to Visualize Human 3-D Object Perception from 2-D Motion

Here, we present an example of a fMRI-weighted MEG inverse procedure in which prior fMRI imaging experiments and a 3-D cortical surface model obtained using structural MRI are used to improve spatial accuracy in the visualization of human brain activity while perceiving 3-D objects from 2-D random-dot motion [10].

Perception of 3-D objects from 2-D motion requires that visual motion is spatially integrated and that the object shape is recognized. Recent neuroimaging studies suggest the involvement of the dorsal (i.e., the parieto-occipital and the intraparietal regions) and the ventral (i.e., the inferior occipito-temporal region) visual systems, as well as the MT area for motion perception, in the perception of 3-D structures from motion [11, 12]. However, the neural dynamics underlying the reconstruction of a 3-D object from 2-D optic flow is not fully understood.

We combined fMRI and MEG data measured during a common cognitive task in which subjects were required to report whether they recognize 3-D objects while seeing random-dot motion in which coherence was parametrically controlled (Figure 1).

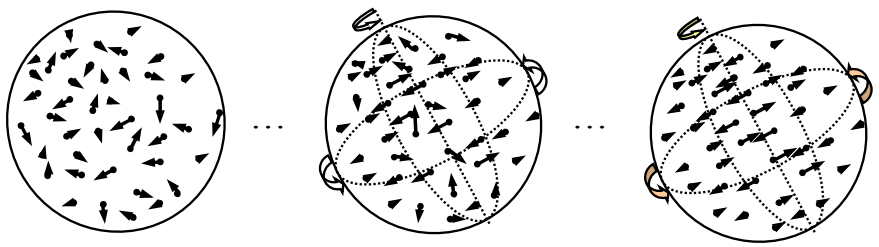

(i) 0 % coherent (random motion) (iii) 60 % coherent (vi) 100 % coherent

Figure 1 Examples of the random-dot motion stimuli used in this study. Coherence of the motion was changed from 0 % to 100 % to generate different 3-D object perception.

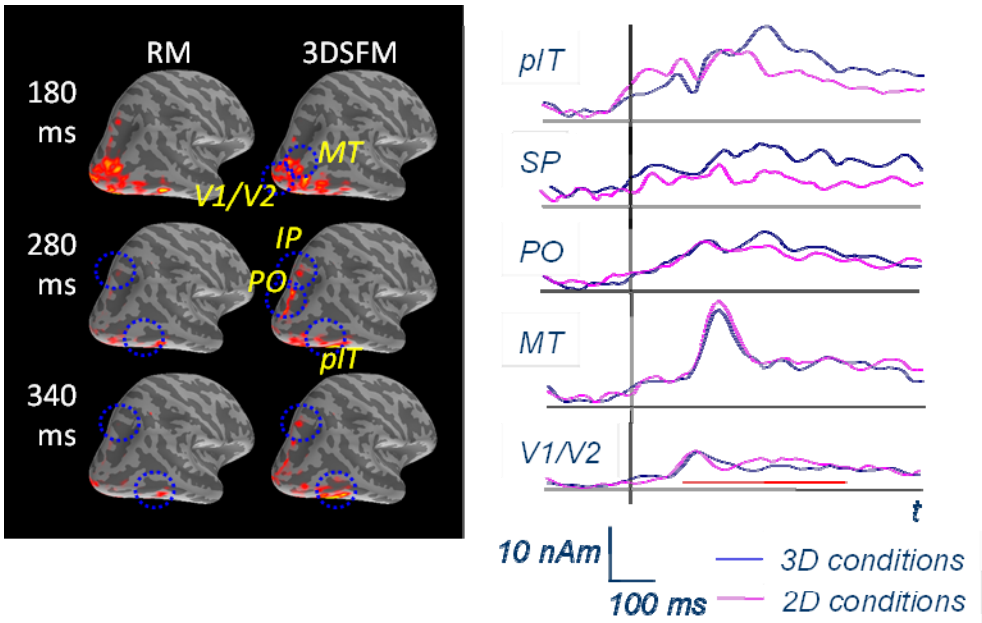

Figure 2 The results of the inter-subject averaging of the activity estimates for random motion (RM: 0 and 20 %) condition and 3-D structure- perception-from-motion (3D-SFM: 80 and 100 %) condition averaged over all seven subjects. The blue circles denote the sites where we observed the major changes between the conditions.

MEG signals were measured while the subjects viewed the moving visual stimuli using a whole-cortex type SQUID system (VECTORVIEW^{TM}, Elekta-Neuromag, Finland) with a band-pass of 0.03 – 150 Hz and sampling rate of 600 Hz. More than 80 epochs were averaged for each condition.

Functional MRI data were collected using a 3-Tesla scanner (Siemens Trio^{TM}, Germany). For functional imaging, single-shot echo-planar imaging (EPI) sequence was used with the imaging parameters TR 3000 ms, TE 40 ms, Flip angle 90 degrees, 40 axial slices, 3 mm thickness with no gap covering the entire brain. Three 14-minute functional scans were divided into 12-second segments, randomly alternating between different stimulus (coherency) conditions and resting (fixation) periods.

3-D reconstruction of the cortical surface was performed using Freesurfer software [13] for each subject. Statistical Parametric Mapping (SPM) was used to infer statistical significance of the signal changes in fMRI data [14]. The results of the fMRI analysis were used to impose plausible constraints on the MEG inverse calculation using a 'weighted' minimum-norm approach to improve spatial resolution of the spatiotemporal activity estimates. In this study, we introduced fMRI weighting, which was determined by thresholding the fMRI statistical parametric map for each condition vs. fixation condition with $p < 0.001$ (False Detection Rate corrected), on the diagonal entries of the source covariance matrix **W** in eq. (3).

Figure 2 shows the results of the fMRI-weighted MEG inverse calculation averaged over all subjects using the spherical morphing technique for inter-subject averaging of the brain activities [15]. Increased neural activity in the parieto-occipital (PO), the intraparietal (IP) and the posterior inferotemporal (pIT) areas were observed only in the 3-D perception (3DSFM) conditions (100 and 80 % coherent conditions) compared to the random motion (RM) conditions (0 and 20 % coherent conditions) in the latencies between 250 and 500 ms after the onset of visual motion.

The present results are in agreement with the previous fMRI studies [11, 12] and add further insight into the temporal characteristics of the neural activities in the inferior temporal and parietal areas during 3-D object perception from motion. The results suggest that the perception of moving 3-D object from 2-D motion includes both perception of global motion and 3-D mental image processing that are accomplished by the cooperative activation in the ventral and dorsal visual pathways.

These results also demonstrate that noninvasive multimodal neuroimaging, in which structural and functional MRI data are incorporated into the MEG inverse problem, is capable of visualizing neural dynamics of the human brain with spatial accuracy comparable to fMRI without compromising the excellent temporal accuracy of MEG. Using the MRI/fMRI incorporated MEG inverse procedure, the time-course of neural activity can be extracted from multiple brain regions-of-interest (ROIs) with millisecond precision. These data could be used to infer neural interactions between various brain regions, which are considered to be crucial neural mechanisms underlying higher order brain functions specific to humans.

4. Conclusion

This paper describes that the spatial accuracy of the MEG inverse problem is enhanced with a priori information of a 3-D cortical structure extracted from structural MR images and possible spatial distribution of brain activation from functional MRI. The MRI/fMRI-incorporated MEG inverse procedure was applied to visualize neural dynamics during 3-D object perception from 2-D motion, which provided new insight into the dynamic interaction between the ventral and dorsal visual information processing streams.

5. References

1. S. Ogawa, T.M. Lee, A.S. Nayak, and P. Glynn, "Oxygenation-sensitive contrast in magnetic resonance image or rodent brain at high magnetic field," *Magn. Reson. Med.*, **14**(1), 1990, pp. 68-78.
2. J.W. Belliveau, D.N. Kennedy, R.C. McKinstry, B.R. Buchbinder, R.M. Weisskoff, M.S. Cohen, J.M. Vevea, T.J. Brady, and B.R. Rosen, "Functional mapping of the human visual cortex by magnetic resonance imaging," *Science*, **254**, 1991, pp. 716-719.
3. M. Hämäläinen, R. Hari, R.J. Ilmoniemi, J. Knuutila, and O.V. Lounasmaa, "Magnetoencephalography--theory, instrumentation, and applications to noninvasive studies of the working human brain," *Rev. Mod. Phys.*, **65**, 1993, pp. 1-93.
4. A.M. Dale and M.I. Sereno, "Improved localization of cortical activity by combining EEG and MEG with MRI cortical surface reconstruction: A linear approach," *J. Cogn. Neurosci.*, **5**(2), 1993, pp. 162-176.
5. A.M. Dale, A.K. Liu, B. Fischl, R. Buckner, J.W. Belliveau, J.D. Lewine, and E. Halgren, "Dynamic statistical parametric mapping: combining fMRI and MEG for high-resolution imaging of cortical activity," *Neuron*, **26**(1), 2000, pp. 55-67.
6. N. Logothetis, J. Pauls, M. Augath, T. Trinath, and A. Oeltermann, "Neurophysiological investigation of the basis of the fMRI signal," *Nature*, **412**, 2001, pp. 150-157.
7. M. Hämäläinen and R.J. Ilmoniemi, "Interpreting magnetic fields of the brain: minimum norm estimates," *Med. Biol. Eng. Comput.*, **32**,1984, pp. 35-42.
8. W. Menke, *Geophysical Data Analysis: Discrete Inverse Theory*. New York, Academic Press, 1984.
9. S. Iwaki, "Multimodal neuroimaging to visualize human visual processing," in J. Wu (eds), *Biomedical Engineering and Cognitive Neuroscience for Healthcare*, IGI Global Press, 2012, pp. 274-282.
10. H. Wallach and D. N. O'Connell, "The kinetic depth effect," *J. Exp. Psychol.*, 1953, **45**, pp. 205-217.
11. G.A. Orban, S. Sunaert, J.T. Todd, P. van Hecke, and G. Marchal, "Human cortical regions involved in extracting depth from motion," *Neuron*, **24**, 1999, pp. 929-940.
12. A.L. Paradis, V. Cornilleau-Peres, J. Droulez, P.F. van de Moortele, E. Lobel, A. Berthoz, D. Le Bihan, and J.B. Poline, "Visual perception of motion and 3-D structure from motion: an fMRI study," *Cereb. Cortex*, **10**, 2000, pp. 772-783.
13. A.M. Dale, B. Fischl, M.I. Sereno, "Cortical surface-based analysis I: segmentation and surface reconstruction.," Neuroimage, **9**, 1999, pp. 179-194.
14. K.J. Friston, "Imaging neuroscience: principles or maps?" *Proc. Natl. Acad. Sci. USA*, **95**, 1998, pp. 796-802.
15. B. Fischl, M.I. Sereno, R.B. Tootell, A.M. Dale, "High-resolution intersubject averaging and a coordinate system for the cortical surface," *Hum. Brain Mapp*., **8**, 1999, pp. 272-84.
16. S. Iwaki, G. Bonmassar, and J.W. Belliveau, "Dynamic cortical activity during the perception of three-dimensional object shape from two-dimensional random-dot motion," *J. Integr. Neurosci.*, **12**, 2013, pp. 355-367.